analytical chemistry

pubs.acs.org/ac Article

Determination of the Isotopic Composition of Aqueous Mercury in a Paddy Ecosystem Using Diffusive Gradients in Thin Films

Hongqian Yin, Heng Yao,* Wei Yuan, Che-Jen Lin, Xuewu Fu, Runsheng Yin, Bo Meng, Jun Luo, and Xinbin Feng*

Cite This: *Anal. Chem.* 2023, 95, 12290−12297 Read Online

ACCESS | Metrics & More | Article Recommendations | Supporting Information

ABSTRACT: Measuring the isotopic composition of Hg in natural waters is challenging due to the ultratrace level of aqueous Hg (ng L^{-1}). At least 5 ng of Hg mass is required for Hg isotopic analysis. Given the low Hg concentration in natural waters, a large volume of water (>10 L) is typically needed. The conventional grab sampling method is time-consuming, laborious, and prone to contamination during transportation and preconcentration steps. In this study, a DGT (diffusive gradients in thin films) method based on aminopropyl and mercaptopropyl bi-functionalized SBA-15 nanoparticles was developed and extended to determine the concentration and isotopic composition of aqueous Hg for the first time. The results of laboratory analysis showed that Hg adsorption by DGT induces ∼ −0.2‰ mass-dependent fractionation (MDF) and little mass-independent fractionation (MIF). The magnitude of MDF exhibits a dependence on the diffusion-layer thickness of DGT. Since Hg-MDF can occur in a broad range of environmental processes, monitoring the δ^{202}Hg of aqueous Hg using the DGT method should be performed with caution. Field results show consistent MIF signatures (Δ^{199}Hg) between the DGT and conventional grab sampling method. The developed DGT method serves as a passive sampling method that effectively characterizes the MIF of Hg in waters to understand the biogeochemical cycle of Hg at contaminated sites.

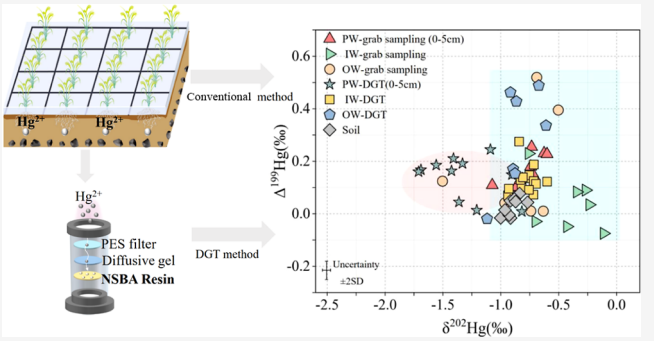

1. INTRODUCTION

Mercury (Hg) is a globally distributed toxic metal regulated by the United Nations Environment Programme (UNEP). It is transported globally in the atmosphere and continuously deposited in terrestrial and aquatic ecosystems.[1,2] The toxicity and environmental risk of Hg largely depend on the chemical speciation of Hg. In aquatic ecosystems, a fraction of Hg is microbially converted to methylmercury (MeHg) and biomagnified by 10^6−10^7 times in the food chain, causing concerns on human health and contamination of ecosystems.[1,3,4] In natural waters, free aqueous Hg(II) and its labile complexes are the most bioavailable Hg species subject to methylation.[5−8] It is crucial to understand the sources, transformation, and distribution of aqueous Hg(II). Stable Hg isotopes undergo mass-dependent fractionation (MDF) (reported as δ^{202}Hg) and mass-independent fractionation (MIF) (reported as Δ^{199}Hg, Δ^{200}Hg, and Δ^{201}Hg).[9] The quantitative values of fractionation serve as useful tracing signals in understanding Hg biogeochemical cycle. Hg-MDF occurs in physical, chemical, and biological processes,[9,10] while Hg-MIF occurs during photochemical reactions,[11−13] abiotic dark reduction and oxidation,[5,13] and equilibrium fractionation.[14]

The methods for determining the isotopic composition of Hg in solid samples (*e.g.*, rock, soil, sediment, and biomass samples) have been well established.[7,15,16] However, the methods for measuring Hg isotopes in natural waters remain less available due to the analytical challenges caused by low concentration (usually at ng L^{-1} levels). The available methods, based on $SnCl_2$ reduction of Hg(II) using a large volume of sample (>10 L) and preconcentration of the produced Hg(0) into a few mL of reverse aqua regia trapping solution,[17] are frequently laborious and time-consuming.[17,18] Water in glass containers are prone to degradation and contamination during the collection, preservation, and transportation of field samples.[19] In addition, grab sampling does not allow longer-term monitoring of transformation processes.[19,20] A method for an effective, low-cost, *in situ* collection of Hg in natural waters for Hg isotope analysis is therefore needed.

Received: March 29, 2023
Accepted: July 27, 2023
Published: August 10, 2023

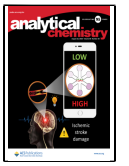

The diffusive gradients in thin films (DGT) technique offers an effective and *in situ* approach to collect, concentrate, and preserve labile trace constituents in water.[8,21−24] This technique reduces the risk of sample contamination caused by post-sampling transport and storage.[25−28] Although it has been successfully used for monitoring the concentration of labile aqueous Hg(II),[8,29] its application in determining the isotopic composition of Hg(II) is not prevalent. Most DGT resins contain thiol (−SH) groups (*e.g.*, Spheron−Thiol, Chelex-100 and 3-mercaptopropyl-functionalized silica) for capturing labile aqueous Hg species because of their strong affinity to Hg(II).[22,30,31] The 3-mercaptopropyl-functionalized silica (3-MFS) resin gel has been used for methylmercury determination.[32−35] Few studies used 3-MFS resin gel to monitor aqueous Hg(II).[36] Others established that DGT resins are either not readily available commercially (*e.g.*, Spheron−Thiol) or exhibit weak adsorption characteristics (*e.g.*, Chelex-100).[8,22,30]

In this study, we developed a novel DGT method for determining the concentration and isotopic composition of aqueous Hg(II). The DGT device was assembled using a binding resin containing aminopropyl and mercaptopropyl bi-functionalized SBA-15 nanoparticles (NSBA, SBA-15 is a mesoporous silica sieve with hexagonal pores and a tunable pore diameter of 5−15 nm). Laboratory experiments were designed to (i) examine the adsorption characteristics of Hg(II) by NSBA-DGT and (ii) determine Hg isotope fractionation during NSBA-DGT adsorption of Hg(II). Field verification was performed at the Wanshan Mercury Mine (WMM) of Guizhou Province in Southwest China. The site was a Hg mining region that experiences legacy Hg contamination in local rice paddies.[34]

2. EXPERIMENTAL SECTION

2.1. Reagents, Solutions, and DGT. Hg(II) standard solutions were prepared from ACS Aladdin standard stock solutions (1000 mg L^{-1} in 1 mol L^{-1} HNO_3). All reagents (HCl, HNO_3, $SnCl_2{\cdot}2H_2O$, $NH_2OH{\cdot}2HCl$, NaCl, and NaOH) were of analytical grade (Sinopharm Chemical Reagent Co., Ltd., China). BrCl solutions were prepared by heating potassium bromate and potassium bromide reagent at 250 °C for 12 h. $NH_2OH{\cdot}2HCl$ solutions (25%, w/v) and $SnCl_2$ solutions (30%, m/v) were prepared following the US EPA Method 1631.[37] NIST SRM 3133 and NIST SRM 8610 Hg were used as the stable Hg isotope standards. NIST SRM 997 thallium (25 ng mL^{-1} in 3% HNO_3) was utilized to enable internal inter-elemental correction of instrumental isotopic fractionation.[18]

NSBA-DGT was purchased from DGT Research Ltd., UK (Serial No: LSNBN-AP). It consists of 0.4 mm thick NSBA resin gel[38] embedded in 1.5% agarose diffusive gel of various thicknesses (0.40 mm, 0.80 mm, and 1.2 mm)[39] and a 0.14 mm-thick polyether sulfone (PES) membrane filter (Pall, U.S.) with 0.45 μm pore size (Figure 1). All plasticware used for analyses was new and cleaned by soaking in 10% HNO_3 (v/v) over 24 h and then rinsed with 18.2 MΩ·cm water (MQ, Millipore, U.S.). NSBA gel and PES membranes were stored in a NaCl (0.01 mol L^{-1}) solution to avoid charge-induced disequilibrium artifacts.[40]

2.2. Laboratory Experiments. Experiments were conducted for (i) elemental analysis of aqueous Hg(II) (detailed description is given in the Supporting Information) and (ii) isotopic analysis of aqueous Hg(II) (described in later sections).

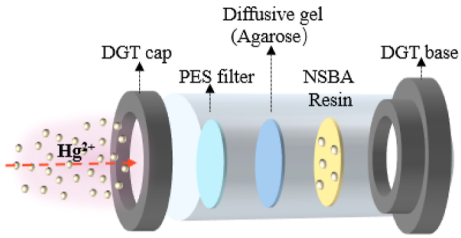

Figure 1. Diagram of the developed DGT unit. The binding gel contains thiol and amino groups that have a large sorption capability for Hg(II). The labile Hg(II) passes through a filter and a diffusive layer and binds with NSBA gel (binding layer).

To determine the temperature effects on Hg isotope fractionation using NSBA-DGT, the NSBA-DGT devices were deployed in 100 mL of Hg(II) (NIST SRM 3133) standard solutions containing ∼60 ng mL^{-1} and 0.01 mol L^{-1} NaCl at 15, 25, and 35 °C (pH = 5). The higher concentration was intended to obtain the isotope fractionation factor during the experiments and accurate Hg isotope analysis. The DGT device deployment time is described as follows: at 15 °C: 4, 6, 8, 12, 16, and 24 h; at 25 °C: 1, 2, 4, 6, 8, 12, and 24 h; at 35 °C: 2, 3, 4, 5, 6, 8, 12, and 24 h. The solutions were placed on a thermostatic oscillator (THZ-98C, YIHENG INSTRUMENTS) at 120 rpm at each temperature. Before the DGT units were separately immersed in the solution, the solution and instrument were maintained at the experimental temperature for 2 h. The DGT units were removed from the solution at each time step and eluted with 5 mL of reverse aqua regia (HCl/HNO_3, 1:3 *v*/*v*) in polytetrafluoroethylene bottles for 8 h at room temperature. Bromine chloride solution (1% *v*/*v*) was added to the residue solutions and stored in a refrigerator (at 4 °C) before the analysis of Hg concentration and isotopic composition. All solutions were placed in the dark to avoid potential photoreduction. Triplicate analyses were conducted for all samples.

NSBA-DGT devices with various thicknesses of diffusion layer (0.4, 0.8, and 1.2 mm) were used for determining the optimal gel thickness in a solution containing 60 ng mL^{-1} Hg(II) and 0.01 mol L^{-1} NaCl for 12 h (pH = 5, T = 25 °C). To study the effects of ionic strength (IS) on Hg isotope fractionation, the NSBA-DGT devices of 0.8 mm gel thickness were immersed in 100 mL of NIST SRM 3133 standard solution containing ∼60 ng mL^{-1} Hg(II) and ISs (0.001, 0.01, 0.1, and 0.5 mol L^{-1} NaCl) for 8 h (pH = 5, T = 25 °C). Treatments of all experiment steps, DGT eluates, and residue solutions are kept the same as the above.

2.3. Field Experiments. We compared the developed NSBA-DGT method with the traditional sampling methods to determine the performance of the DGT method in the field. Three field sampling campaigns of 20−40 days, 40−60 days, and 60−80 days were conducted after the planting of rice in a rice paddy of the Gouxi area, WMM, from July to September 2021. Before field deployment, the DGT devices were stored in a 0.01 mol L^{-1} NaCl solution. In each campaign, the DGT devices were deployed *in situ* to sample irrigation water (IW) (n = 30), overlying water (OW) (0.5 cm below water surface, n = 30), and pore water (PW) in the root zone (0−15 cm in soil, n = 5) in the paddy field for 2 weeks. The concentration of Hg(II) at the site is at ng L^{-1} level.[4,41] To obtain sufficient Hg

https://doi.org/10.1021/acs.analchem.3c01356
Anal. Chem. 2023, 95, 12290−12297

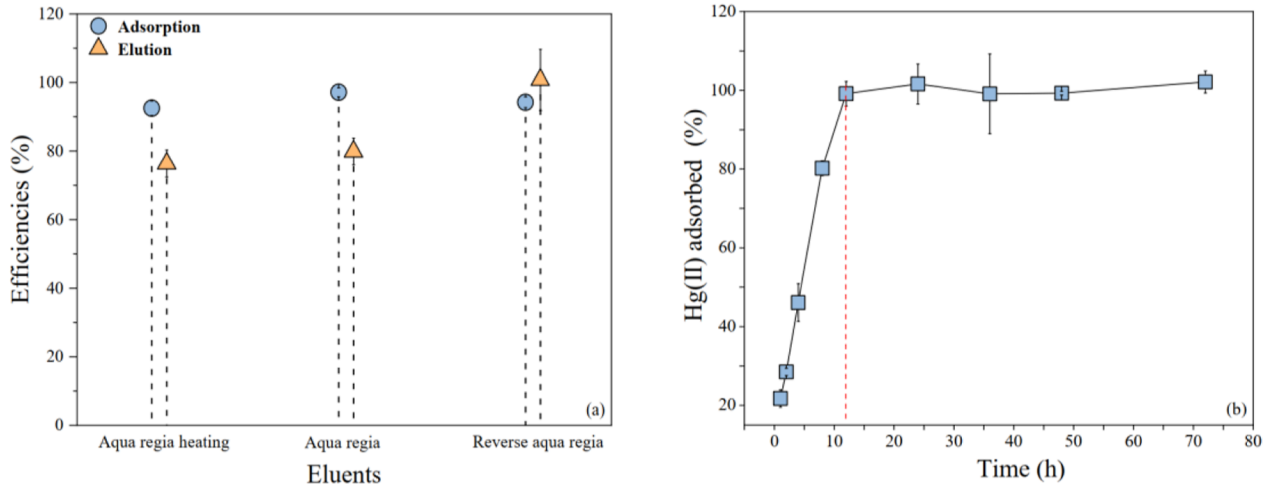

Figure 2. Elution efficiency and uptake of Hg(II) by the NSBA gel. (a) Elution efficiencies of Hg(II) bound to the NSBA gel and then eluted with eluents. (b) Uptake of Hg(II) over time by the NSBA gel immersed in 30 mL of 0.01 mol L^{-1} NaCl solutions containing 1 ng mL^{-1} Hg(II) (room temperature, pH = 5). Error bars represent standard deviations of replicates (n = 3).

mass (>5 ng) for isotope analysis and ensure analytical precision, 3−4 DGT samples were combined and eluted in one composite sample for IW and OW. After sampling, the DGT devices were rinsed thoroughly with 18.2 MΩ·cm water on-site and carried back for laboratory analysis as described in the Laboratory Experiments Section. In each campaign, two new DGT samplers were taken to the field and kept assembled in a clean bag to obtain DGT blanks. Those DGT units were exposed to the 0.01 mol L^{-1} NaCl solution for 24 h and then transported back to the laboratory for analysis.

For comparison, 4 L of IW, OW, and PW was directly sampled on the 40th, 60th, and 80th day after the planting of rice using precleaned borosilicate glass bottles. The PW samples were collected after centrifugation (2850 × g for 20 min), and all water samples were filtered [0.45 μm Mixed Cellulose Esters (MCE) membrane filtration] on-site. Then, 0.4% HCl and 1% BrCl (v/v) were added to the water samples to oxidize all Hg species to Hg(II), followed by a Hg preconcentration procedure described in our earlier work.[17] The trapping solutions were stored in a refrigerator at 4 °C before Hg concentration and Hg isotope analysis.

Rhizosphere soil samples were also collected on the 40th, 60th, and 80th day from the root zone (0−15 cm). Soils were collected in triplicate at three sites (n = 9) by hand with disposable polyethylene gloves, sealed in clean polyethylene bags, and then shipped to the laboratory, freeze-dried (−78 °C), ground to 200 mesh, homogenized, sealed in plastic bags, and stored at room temperature.[4,42,43] All soil samples were digested with 5 mL of aqua regia (HCl/HNO_3, 3:1 v/v) as described in our earlier work.[4,44] The digested soil solutions were stored in a refrigerator (at 4 °C) before Hg concentration and isotopic composition analyses. The temperatures of rhizosphere soil were recorded at 30 min intervals throughout the experiment by a single-layer soil moisture temperature tester (TPFS-WS-1, Shanghai, China), and water pH was determined by a pH meter (YSI ProQuatro, USA) before the DGT deployment (Table S1).

2.4. Analysis of Hg Concentration and Isotopic Composition. The concentrations of Hg(II) of all solutions were measured using a cold vapor atomic fluorescence spectrophotometer (model 2500, Tekran Instruments, Canada) or a cold vapor atomic absorption spectrometer (F732-S, Huaguang, China).[45,46] Acid digestion of a soil standard reference material (GBW07405, 290 ng g^{-1} Hg, IGGE), treated in the same way as the soil samples, yielded Hg recoveries of 98.6 ± 2.4% (SD, n = 2).

The Hg isotopic composition of the sample solutions was measured using a multi-collector inductively coupled plasma mass spectrometer (Neptune II, Thermo Scientific, USA) coupled with a gas/liquid separation system. Hg isotope values were measured and calculated following a previously reported method.[47,48] The analytical details of Hg isotope measurements are described in Supporting Information (Section S6). The analytical uncertainty (2σ) in the isotopic composition of sample was determined by the larger values of the analysis of either replicated samples or secondary standards.

2.5. Mercury Mass Balance Model. A Hg mass balance model was applied to assess data quality. The model assumes that DGT immobilizes aqueous Hg in the binding layer (NSBA gel) in a closed system and that the process is irreversible (Figure S1). As a result, the Hg isotopic compositions of residual reactants (as $Hg_{residue}$) and products (DGT, as $Hg_{adsorbed}$) can be described as follows

$$\delta^{202}Hg_{initial} = f \times \delta^{202}Hg_{residue} + (1 - f) \times \delta^{202}Hg_{absorbed} \quad (1)$$

The isotopic difference of Hg adsorbed on the DGT and Hg in initial solutions, the $\varepsilon^{202}Hg_{adsorbed\text{-}initial}$, was calculated as follows

$$\varepsilon^{202}Hg_{absorbed-initial} = \delta^{202}Hg_{adsorbed} - \delta^{202}Hg_{initial} \quad (2)$$

where $\delta^{202}Hg_{initial}$ represents the theoretical initial $\delta^{202}Hg$ of the solution, f is the fraction of the Hg residual reactant, (1 − f) is the fraction of adsorbed Hg on DGT, and $\delta^{202}Hg_{residue}$ and $\delta^{202}Hg_{adsorbed}$ are the measured $\delta^{202}Hg$ values in the residual reactant and the analyte adsorbed on DGT, respectively.

2.6. DGT Blank and Statistical Analysis. The average DGT blank values were 0.05 ± 0.01 ng $disk^{-1}$ (mean ± SD, n = 9). Since Hg isotope analysis requires no less than 5 ng of Hg, the DGT blank was negligible (<5% Hg in each sample). The method detection limits (MDLs = 3 × standard deviations of DGT blanks) and method quantification limits (MQLs = 10 × standard deviations of DGT blanks) were 4.96 ng L^{-1} (0.03

https://doi.org/10.1021/acs.analchem.3c01356
Anal. Chem. 2023, 95, 12290−12297

ng disc^{-1}) and 16.53 ng L^{-1} (0.10 ng disc^{-1}), respectively, for a DGT deployment of 24 h at 25 °C. If the Hg(II) concentration is lower than the MDLs, a longer deployment time and thinner diffusive gels can be used to increase the accumulated mass on the binding gels to lower the MDLs proportionately.[49] Statistical analysis and hypothesis tests were performed using Origin 2020 software using a significance level of 0.05 if not otherwise stated.

3. RESULTS AND DISCUSSION

3.1. Elution Efficiency. The elution efficiencies of the NSBA binding gel using various eluents are shown in Figure 2a. It is clear that aqua regia is an adequate eluent for concentration measurements but at a lower elution efficiency compared to that of reverse aqua regia (76.4−79.9% with 5 mL of pure aqua regia in a 95 °C water bath for 3 h or at 25 °C for 8 h). High elution efficiencies of 100.8 ± 8.9% were obtained using 5 mL of pure reverse aqua regia (HCl/HNO_3, 1:3 v/v) for 8 h at room temperature (Figure 2a). The high effectiveness of reverse aqua regia may be due to its stronger oxidation capability to break the Hg(II)−thiol complex and Hg(II)−amino complex.[50]

3.2. Hg Adsorption. As shown in Figure 2b, the Hg mass adsorbed by the binding gels increased linearly with respect to time in the first 10 h and then remained relatively unchanged. After 12 h, the adsorption efficiency by NSBA gel disks reached 99%. Figure 2b shows that the uptake flux of NSBA gel over the first hour was 0.02 ng min^{-1} cm^{-2} (calculated by eq S2) in a 1 ng mL^{-1} Hg standard solution (~30 ng). The diffusive flux measured in this study is lower than that reported by Pi et al.,[8] which had a higher concentration of aqueous Hg(II) that enhances the diffusive flux because of the greater concentration gradient.[8] In a 1 ng mL^{-1} Hg solution, the diffusion flux of NSBA-DGT for Hg(II) (0.005 ng min^{-1} cm^{-2}) agrees with the value of the DNA-DGT sensor reported by Pi et al. (0.006 ng min^{-1} cm^{-2}).[8] Moreover, Hg(II) uptake by the NSBA binding gel is much faster than the diffusive transport in NSBA-DGT, implying that the DGT device acts as a complete substrate sink. The concentration at the interface between the binding gel and the diffusive gel approaches zero, and therefore, the Hg(II) concentration in solution can be accurately estimated by eq S3.[51−53]

3.3. Diffusion Coefficient. The diffusion coefficient (D_{DGT}) of Hg(II) was determined to calculate the concentration measured by DGT. As shown in Figure S2, the mass of Hg(II) diffused into the binding gel increased linearly with respect to time ($R^2 > 0.999$, $p < 0.01$, ANOVA). The estimated D_{DGT} for Hg(II) calculated using eq S3 was 7.56 (±0.61) × 10^{-6} cm^2 s^{-1} at 25 °C, consistent with previously reported values (6.19 × 10^{-6} cm^2 s^{-1} ~ 7.8 × 10^{-6} cm^2 s^{-1}).[30,54−56] The diffusion coefficients of Hg(II) in NSBA gel at different temperatures were calculated using eq S4.

3.4. Time-Dependent Hg Accumulation by NSBA-DGT. The DGT sampling performance depends on the accumulation capacity of the DGT samplers.[57] As shown in Figure S3, at pH 5, 25 °C and in the first 24 h of sorption time, the mass of Hg(II) in NSBA-DGT increased linearly with respect to time ($R^2 > 0.999$, $p < 0.001$, ANOVA). The DGT-measured Hg masses were consistent with the value predicted by eq S3, with a $M_{measured}/M_{predicted}$ ratio of 0.97 ± 0.05 (mean ± SD). The mass fractions adsorbed by DGT at 48 and 72 h were 31.12 ± 1.47 and 42.87 ± 2.82% of the total available Hg mass in the solution, respectively. Hg(II) was continually consumed in the aqueous phase. The Hg(II) sorption rate gradually slowed because of the lowered concentration gradient over time, which caused the measured line to deviate from the theoretical uptake line. Although the capacity is considered crucial for accurate isotope ratio analysis by DGT,[58] given the levels of Hg(II) at ng L^{-1} (0.2−20 ng L^{-1}) in the natural environment[17] and the accumulation of Hg(II) mass being greater than 2500 ng per gel disk (2.5 cm in diameter) (Figure S3), the NSBA-DGT was sufficient to capture Hg(II) in the concentration range typically encountered at remote and contaminated sites.

3.5. Effect of pH and IS. Both pH and IS in the aqueous solution can potentially affect DGT performance and sorption rate by changing the chemical speciation in the solution.[59−61] In the absence of competing ions and coordinating ligands and colloids, the concentrations of analytes measured by DGT (C_{DGT}) and the actual solution concentrations (C_{soln}) are comparable, with a C_{DGT}/C_{soln} (R) ratio of 0.9−1.1.[60,62] As shown in Table 1, a change in pH from 4.17 to 8.88 neither significantly alters the C_{DGT}/C_{soln} ratio (1.06−0.94) nor changes the salinity from 0.001 to 0.5 mol L^{-1} NaCl (C_{DGT}/C_{soln} ratio = 0.94 to 1.04). The pH of natural waters typically ranges from 3 to 8,[40] with an IS in the range from 0.01 to 0.5 mol L^{-1}.[59] Our results thus indicate that the NSBA-DGT device is capable of measuring aqueous Hg(II) concentrations under environmental pH and IS.

Table 1. Effects of pH and Ionic Strength on Hg(II) Uptake by NSBA-DGT (T = 25 °C for 8 h Adsorption)

pH	NaCl (mol L^{-1})	C_{DGT} (μg L^{-1})	C_{soln} (μg L^{-1})	C_{DGT}/C_{soln}
5	0.001	54.80±1.12	55.07±0.69	1.00±0.01
5	0.01	57.28±4.31	55.33±0.72	1.04±0.09
5	0.1	54.80±2.97	53.98±0.34	1.01±0.05
5	0.5	50.92±1.12	53.97±0.70	0.94±0.03
4.17	0.01	56.16±0.00	52.88±0.00	1.06±0.00
5.96	0.01	52.24±1.96	53.29±0.71	0.98±0.05
8.88	0.01	26.06±1.42	27.86±0.00	0.94±0.05

3.6. Isotope Fractionation of Hg during DGT Sampling. The MDF (δ^{202}Hg) in the residual reactant and DGT product is shown in Figure 3a−c. The δ^{202}Hg values of NSBA-DGT-adsorbed Hg ($\delta^{202}Hg_{adsorbed}$: −0.36‰ to −0.08‰) are consistently more negative compared to that of initial solution ($\delta^{202}Hg_{initial}$: ~0‰), suggesting that lighter Hg isotopes were preferentially adsorbed by DGT (Figure 3a−c). This resulted in the slightly heavy Hg isotopes in the residue solution as $\delta^{202}Hg_{residue} > 0$ (0.05 ± 0.04, 0.02 ± 0.06, and 0.05 ± 0.04‰ at 15, 25, and 35 °C, respectively, $p > 0.05$ by independent t-test) (Figure 3a−c). The average isotopic fractionation factors ($\varepsilon^{202}Hg_{adsorbed\text{-}initial}$) of the initial solutions ($\delta^{202}Hg_{initial}$) and NSBA-DGT ($\delta^{202}Hg_{adsorbed}$) were −0.18 ± 0.05, −0.20 ± 0.06,, and −0.15 ± 0.06‰ at 15, 25, and 35 °C, respectively (Figure 3a−c and Table S3). Although the adsorption efficiency showed an increase with respect to the temperature, the difference in $\varepsilon^{202}Hg_{adsorbed\text{-}initial}$ values is insignificant in all experiments (average value: −0.18 ± 0.06‰, n = 63; Table S3; $p > 0.05$, ANOVA). The MDF values may also vary depending on the water chemistry of Hg(II) in the water sample. For all temperatures, the calculated $\delta^{202}Hg_{initial}$ values agree with the δ^{202}Hg of the solution of NIST SRM 3133, suggesting that Hg isotopic mass is mass-conserved (Figure 3a−c). No MIF was observed

https://doi.org/10.1021/acs.analchem.3c01356
Anal. Chem. 2023, 95, 12290−12297

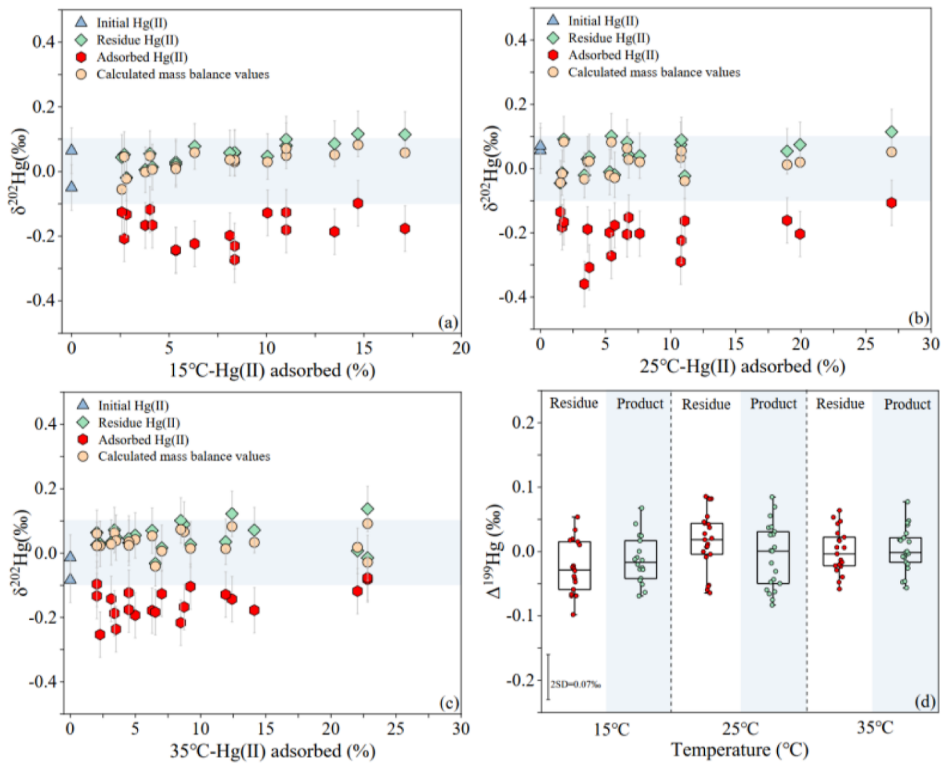

Figure 3. (a−c) Mass balance of stable Hg isotopes for experiments performed at 15, 25, and 35 °C. The red points represent the isotope values of product (DGT); green points represent the isotope values of residue (reactant), and orange points/light blue shaded area is the range of theoretically calculated isotope mass balance values. (d) MIF (Δ^{199}Hg) values of reactants (residue) and products (DGT) at different temperatures. White bands are Δ^{199}Hg values of residue solution, and light blue bands are Δ^{199}Hg values of DGT. Error bars on the *Y*-axis are analytical uncertainties of δ^{202}Hg and Δ^{199}Hg as defined in the Experimental Section (NIST SRM 8610).

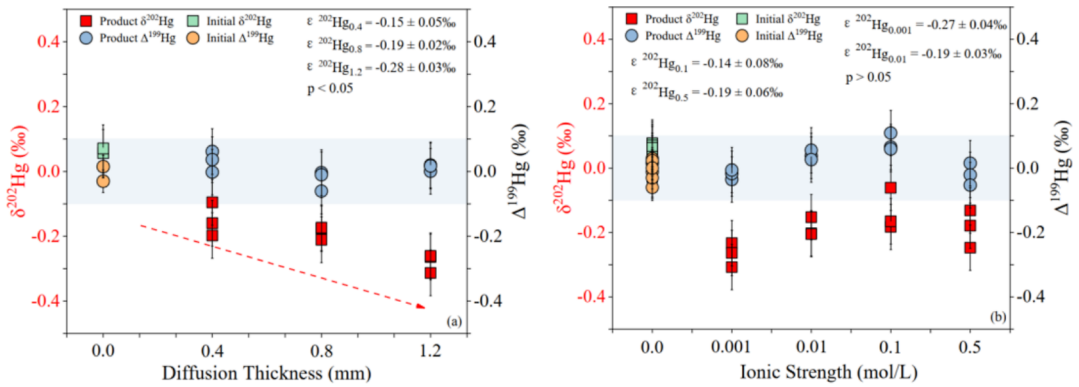

Figure 4. Measured values of Δ^{199}Hg (MIF) and δ^{202}Hg (MDF) at various diffusion thicknesses and ISs. (a) Hg isotope composition of the initial solution and the isotopic fractionation (Δ^{199}Hg and δ^{202}Hg) caused by the diffusion-layer thickness (0.4 mm, 0.8 mm, and 1.2 mm). (b) Hg isotope composition of the initial solution and the isotope fractionations (Δ^{199}Hg and δ^{202}Hg) caused by the ionic strength (0.001, 0.01, 0.1, and 0.5 mol L^{-1} NaCl). Error bars on the *Y*-axis are analytical uncertainties of δ^{202}Hg and Δ^{199}Hg as defined in the Experimental Section (NIST SRM 8610).

during the experiments at all temperatures (Figure 3d and Table S3), indicating the sampling capability of the DGT method for measuring Δ^{199}Hg and Δ^{201}Hg in natural water samples.

The extent of Hg adsorption was 0∼25% in this experimental set (Figure 3a−c). The deviation of δ^{202}Hg between DGT-sampled Hg and the initial Hg(II) solution (∼0‰) decreased slightly when the extent of Hg adsorption reached ∼25% at 25 and 35 °C (Figure 3b,c). During field sampling, the aqueous Hg(II) concentration should show little change because of the abundance of Hg(II) in the environment and a continuous supply of Hg(II) due to water flow. Therefore, 0−25% covers the typical concentration range sufficiently.

3.7. Effect of Diffusion-Layer Thickness on Isotope Fractionation. At pH 5 and 25 °C, DGT devices of various diffusion-layer thicknesses (*i.e.*, agarose gel thicknesses of 0.4, 0.8, and 1.2 mm) were utilized to quantify the influence of diffusive thickness on isotope fractionation. As shown in Figure S4, the measured Hg mass (M, calculated using eq S1) accumulated on the NSBA gel is inversely proportional to the diffusion-layer thickness (Δg). Figure 4a and Table S4 show that the Hg adsorbed by DGT exhibited zero Δ^{199}Hg and Δ^{201}Hg, suggesting that Hg-MIF did not occur (p > 0.05,

https://doi.org/10.1021/acs.analchem.3c01356
Anal. Chem. 2023, 95, 12290−12297

independent-samples *t*-test). However, the δ^{202}Hg value of Hg adsorbed onto DGT decreased with the thickness of the diffusion layer as expected, from −0.15 ± 0.05‰ at 0.4 mm, −0.19 ± 0.02‰ at 0.8 mm, to −0.28 ± 0.03‰ at 1.2 mm (p < 0.05, ANOVA). The diffusion rates at a thicker diffusion layer were slower because of the greater diffusion distance. A value of 0.8 mm was selected a standard diffusion gel thickness for subsequent experiment because the thickness is a good fit in the DGT device enclosure with a 0.4 mm binding gel and a 0.14 mm membrane filter.[63]

3.8. Effects of IS on Hg Isotope Fractionation. Experiments using solutions of NaCl concentration from 0.001 to 0.5 mol L^{-1} with a constant Hg(II) concentration (~60 ng mL^{-1}) were performed to examine the effect of IS on Hg isotope fractionation during DGT sampling (pH = 5, T = 25 °C). Insignificant difference in the δ^{202}Hg values of DGT ($\delta^{202}Hg_{adsorbed}$) was found (Figure 4b) (p > 0.05, ANOVA). No discernible electrostatic effects were observed because the uptake of Hg(II) by the DGT device is driven by diffusion.[63] Figure 4b and Table S5 illustrate consistent DGT Δ^{199}Hg and Δ^{201}Hg values (~0‰) in the tested IS range, suggesting that water salinity may not shift MDF and MIF values.

3.9. Field Application in Flooded Paddies. Total Hg (THg) concentrations of paddy soils were 20.8 ± 2.33 μg g^{-1} (SD, n = 9). The Hg(II) concentrations measured by the developed DGT method, and by the grab sampling method using 0.45 μm MCE membrane filtration, in IW, OW, and PW were compared (Table S6). The Hg(II) concentrations in IW and OW determined by the DGT method were lower than the values determined by the grab sampling method. This result was caused by two reasons. One is that the DGT membrane was gradually clogged by the suspended particulate matter, and therefore, the diffusion of Hg across the membrane was limited over time. Second, the sorption efficiency obtained in the lab was likely higher than that in the field because of the formation of Hg(II)−DOM complexes that lowered the diffusion coefficient due to the increased mass of Hg(II)-DOM complexes.[36] However, the concentration difference does not affect the Hg−MIF signals. The C_{DGT}/C_{soln} ratios ranged from 0.12 to 0.22 in PW, consistent with previously reported values of Sr determined in a soil solution.[40] The low ratio was mainly due to the slow replenishment of Hg(II) in the aqueous phase from the soil solid phase.[40,64]

The isotopic compositions of IW, OW and PW collected by DGT and grab samples are shown in Figure 5 and Table S7. The Δ^{199}Hg values of each water sample from the two sampling methods were comparable using the DGT and grab sampling method: 0.12 ± 0.05 *versus* 0.05 ± 0.10‰ for IW (p = 0.10, independent-samples *t*-test); 0.17 ± 0.19 *versus* 0.18 ± 0.22‰ for OW (p = 0.38, independent-samples *t*-test); and 0.14 ± 0.08 *versus* 0.16 ± 0.06‰ for PW (p = 0.47, independent-samples *t*-test). The comparable Δ^{199}Hg values among the water samples suggest that the dissolved Hg could share the same source.

The δ^{202}Hg values of Hg(II) measured by DGT in IW (δ^{202}Hg: −0.79 ± 0.09‰, SD, n = 15) were comparable to the value of OW (δ^{202}Hg: −0.85 ± 0.29‰, SD, n = 7) (p = 0.38, independent-samples *t*-test), but different from that in PW (δ^{202}Hg: −1.32 ± 0.29‰, SD, n = 11) (p < 0.01, independent-samples *t*-test). The δ^{202}Hg values of grab samples were more consistent with each other for IW (−0.45 ± 0.26‰, SD, n = 8), OW (−0.84 ± 0.36‰, SD, n = 6), and PW (−0.78 ± 0.14‰, SD, n = 9) (p > 0.05, independent-samples *t*-test). The

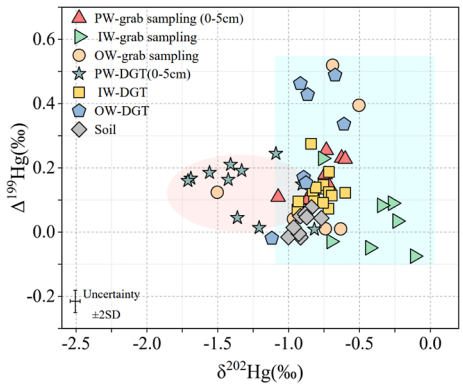

Figure 5. Δ^{199}Hg (MIF) and δ^{202}Hg (MDF) values in IW, OW, and PW collected by the grab sampling and DGT method and soil samples from the Gouxi Artisanal Hg Mining Site. The light blue shaded area shows the region of IW/OW isotopic signatures measured by the DGT method, whereas the light red shaded area shows the region of PW isotopic signatures. Error bars on the *Y*-axis are analytical uncertainties of δ^{202}Hg and Δ^{199}Hg as defined in the Experimental Section (NIST SRM 8610).

variation in δ^{202}Hg values between the DGT and grab sampling methods differed from the variation measured in laboratory experiments. Since Hg-MDF takes place in a wide variety of physical, chemical, and biological processes, such differences could be that the labile Hg(II) sampled by the DGT method represents a fraction of the total dissolved Hg, and the partial sampling causes a MDF shift. In addition, the common ion effect caused by multiple metal cations and complexing ligands (*e.g.*, chloride, sulfate, phosphate, and DOC) could also bias the sampling of DGT for MDF signals.[63,65,66]

It is important to note that the DGT sampling technique measures *in situ*, time-averaged concentration and isotopic composition of Hg(II) for the entire deployment period. Therefore, it is possible to design the measurement periods to capture the signals for the processes of interest, especially tracing the processes that cause Δ^{199}Hg shifts. As shown in Figures 5 and S5, more positive Δ^{199}Hg values were detected by the DGT method in the OW than in the IW and PW samples and soils, which showed near-zero values. This is because the OW underwent photoreduction, particularly in the early growing season when there was weak light shielding of the small rice plants. The photoreduction became weaker in the later growth stage with increased rice leaf area that provided shielding of solar irradiance.

4. CONCLUSIONS

Data for the isotopic composition of Hg in natural waters remain relatively scarce. In this study, we developed a DGT method for measuring the isotopic composition of aqueous Hg(II) with a low procedure blank (0.05 ± 0.01 ng $disk^{-1}$, SD, n = 9, <5% Hg mass in the sample). Our data indicate that diffusion-based sampling of Hg isotopes by the DGT method causes a small Hg-MDF (~-0.2‰) but has little impact on Hg-MIF. This method opens the possibility of determining the Hg-MIF signal in water samples at Hg-contaminated sites. The conventional grab sampling method provides data of the isotopic composition of Hg(II) in water at the sampling time[20] and therefore can be affected by the transient variation of aqueous Hg(II). The developed DGT method has the advantage of providing the time-average concentration and MIF of aqueous Hg(II), both are important to advance the

https://doi.org/10.1021/acs.analchem.3c01356
Anal. Chem. 2023, 95, 12290−12297

understanding of the biogeochemical transformation of dissolved Hg(II).

■ ASSOCIATED CONTENT

Supporting Information

The Supporting Information is available free of charge at https://pubs.acs.org/doi/10.1021/acs.analchem.3c01356.

Additional experimental details and datasets and additional figures (PDF)

■ AUTHOR INFORMATION

Corresponding Authors

Heng Yao − *State Key Laboratory of Environmental Geochemistry, Institute of Geochemistry, Chinese Academy of Sciences, Guiyang 550081, China*; Email: yaoheng@mail.gyig.ac.cn

Xinbin Feng − *State Key Laboratory of Environmental Geochemistry, Institute of Geochemistry, Chinese Academy of Sciences, Guiyang 550081, China; University of Chinese Academy of Sciences, Beijing 100049, China*; orcid.org/0000-0002-7462-8998; Phone: +86-851-85895728; Email: fengxinbin@vip.skleg.cn

Authors

Hongqian Yin − *State Key Laboratory of Environmental Geochemistry, Institute of Geochemistry, Chinese Academy of Sciences, Guiyang 550081, China; University of Chinese Academy of Sciences, Beijing 100049, China*

Wei Yuan − *State Key Laboratory of Environmental Geochemistry, Institute of Geochemistry, Chinese Academy of Sciences, Guiyang 550081, China*; orcid.org/0000-0003-3329-2081

Che-Jen Lin − *Center for Advances in Water and Air Quality, Lamar University, Beaumont, Texas 77710, United States*

Xuewu Fu − *State Key Laboratory of Environmental Geochemistry, Institute of Geochemistry, Chinese Academy of Sciences, Guiyang 550081, China*; orcid.org/0000-0002-5174-7150

Runsheng Yin − *State Key Laboratory of Ore Deposit Geochemistry, Institute of Geochemistry, Chinese Academy of Sciences, Guiyang 550081, China*

Bo Meng − *State Key Laboratory of Environmental Geochemistry, Institute of Geochemistry, Chinese Academy of Sciences, Guiyang 550081, China*; orcid.org/0000-0002-7827-8673

Jun Luo − *State Key Laboratory of Pollution Control and Resource Reuse, School of the Environment, Nanjing University, Jiangsu 210023, China*; orcid.org/0000-0002-3480-8900

Complete contact information is available at: https://pubs.acs.org/10.1021/acs.analchem.3c01356

Notes

The authors declare no competing financial interest.

■ ACKNOWLEDGMENTS

This work was supported by the National Natural Science Foundation of China (42177445, 41931297, and 41921004), National Key Research and Development Program of China (2020YFC1807304), and Provincial 2021 Science and Technology Subsidies (no. GZ2021SIG). We thank Kun Zhang for his help in sample collection and measurement and Yang Tang and Guangyi Sun for their help in operating the MC-ICP-MS instrument, from the Institute of Geochemistry, Chinese Academy of Sciences.

■ REFERENCES

(1) Engstrom, D. R. *PNAS* **2007**, *104*, 16394−16395.
(2) Yin, R. S.; Feng, X. B.; Li, X. D.; Yu, B.; Du, B. Y. *Trends Environ. Anal. Chem.* **2014**, *2*, 1−10.
(3) Wang, X.; Ye, Z. H.; Li, B.; Huang, L. N.; Meng, M.; Shi, J. B.; Jiang, G. B. *Environ. Sci. Technol.* **2014**, *48*, 1878−1885.
(4) Qin, C. Y.; Du, B. Y.; Yin, R. S.; Meng, B.; Fu, X. W.; Li, P.; Zhang, L. M.; Feng, X. B. *Environ. Sci. Technol.* **2020**, *54*, 14334−14342.
(5) Zheng, W.; Demers, J. D.; Lu, X.; Bergquist, B. A.; Anbar, A. D.; Blum, J. D.; Gu, B. *Environ. Sci. Technol.* **2019**, *53*, 1853−1862.
(6) Li, P.; Feng, X. B.; Shang, L. H.; Qiu, G. L.; Meng, B.; Zhang, H.; Guo, Y. N.; Liang, P. *Ecotox Environ Safe* **2011**, *74*, 473−479.
(7) Li, P.; Du, B. Y.; Maurice, L.; Laffont, L.; Lagane, C.; Point, D.; Sonke, J. E.; Yin, R. S.; Lin, C. J.; Feng, X. B. *Environ. Sci. Technol.* **2017**, *51*, 12321−12328.
(8) Pi, K. F.; Liu, J. W.; Van Cappellen, P. *Environ. Sci. Technol.* **2020**, *54*, 13680−13689.
(9) Blum, J. D.; Sherman, L. S.; Johnson, M. W. *Annu. Rev. Earth Planet. Sci.* **2014**, *42*, 249−269.
(10) Kritee, K.; Barkay, T.; Blum, J. D. *Geochim. Cosmochim. Acta* **2009**, *73*, 1285−1296.
(11) Zhao, H. F.; Meng, B.; Sun, G. Y.; Lin, C. J.; Feng, X. B.; Sommar, J. *Environ. Sci. Technol.* **2021**, *55*, 13376−13386.
(12) Sun, G. Y.; Sommar, J.; Feng, X. B.; Lin, C. J.; Ge, M. F.; Wang, W. G.; Yin, R. S.; Fu, X. W.; Shang, L. H. *Environ. Sci. Technol.* **2016**, *50*, 9232−9241.
(13) Zheng, W.; Hintelmann, H. *Geochim. Cosmochim. Acta* **2009**, *73*, 6704−6715.
(14) Wiederhold, J. G. *Environ. Sci. Technol.* **2015**, *49*, 2606−2624.
(15) Smith, C. N.; Kesler, S. E.; Blum, J. D.; Rytuba, J. J. *Earth Planet. Sci. Lett.* **2008**, *269*, 399−407.
(16) Yu, B.; Fu, X. W.; Yin, R. S.; Zhang, H.; Wang, X.; Lin, C. J.; Wu, C. S.; Zhang, Y. P.; He, N. N.; Fu, P. Q.; Wang, Z. Y.; Shang, L. H.; Sommar, J.; Sonke, J. E.; Maurice, L.; Guinot, B.; Feng, X. B. *Environ. Sci. Technol.* **2016**, *50*, 9262−9269.
(17) Li, K.; Lin, C. J.; Yuan, W.; Sun, G. Y.; Fu, X. W.; Feng, X. B. *J. Anal. At. Spectrom.* **2019**, *34*, 2303−2313.
(18) Liu, Y. L.; Chen, J. B.; Liu, J. F.; Gai, P. X.; Au Yang, D.; Zheng, W.; Li, Y. B.; Li, D.; Cai, H. M.; Yuan, W.; Li, Y. S. *Anal. Chem.* **2021**, *93*, 15905−15912.
(19) Wang, R.; Biles, E.; Li, Y.; Juergens, M. D.; Bowes, M. J.; Jones, K. C.; Zhang, H. *Environ. Sci. Technol.* **2020**, *54*, 11155−11164.
(20) Desaulty, A. M.; Méheut, M.; Guerrot, C.; Berho, C.; Millot, R. *Chem. Geol.* **2017**, *450*, 122−134.
(21) Pan, Y.; Guan, D. X.; Zhao, D.; Luo, J.; Zhang, H.; Davison, W.; Ma, L. Q. *Environ. Sci. Technol.* **2015**, *49*, 14267−14273.
(22) Gao, Y.; De Canck, E.; Leermakers, M.; Baeyens, W.; Van Der Voort, P. *Talanta* **2011**, *87*, 262−267.
(23) Gao, Y.; De Craemer, S.; Baeyens, W. *Talanta* **2014**, *120*, 470−474.
(24) Zhou, C. Y.; Guan, D. X.; Williams, P. N.; Luo, J.; Ma, L. Q. *Water Res.* **2016**, *99*, 200−208.
(25) Mills, G. A.; Gravell, A.; Vrana, B.; Harman, C.; Budzinski, H.; Mazzella, N.; Ocelka, T. *Environ. Sci.: Processes Impacts* **2014**, *16*, 369−373.
(26) Morin, N.; Miège, C.; Coquery, M.; Randon, J. *TrAC, Trends Anal. Chem.* **2012**, *36*, 144−175.
(27) Seethapathy, S.; Gorecki, T.; Li, X. *J. Chromatogr. A* **2008**, *1184*, 234−253.
(28) Chen, W.; Li, Y.; Chen, C. E.; Sweetman, A. J.; Zhang, H.; Jones, K. C. *Environ. Sci. Technol.* **2017**, *51*, 13274−13281.
(29) Yao, H.; Zhao, Y.; Lin, C. J.; Yi, F.; Liang, X.; Feng, X. *Chemosphere* **2020**, *251*, 126231.

(30) Reichstadter, M.; Gao, Y.; Divis, P.; Ma, T.; Gaulier, C.; Leermakers, M. *Chemosphere* **2021**, *263*, 128320.
(31) Divis, P.; Szkandera, R.; Brulik, L.; Docekalova, H.; Matus, P.; Bujdos, M. *Anal. Sci.* **2009**, *25*, 575−578.
(32) Clarisse, O.; Hintelmann, H. *Journal of Environmental Monitoring* **2006**, *8*, 1242.
(33) Clarisse, O.; Foucher, D.; Hintelmann, H. *Environ. Pollut.* **2009**, *157*, 987−993.
(34) Liu, J. L.; Feng, X. B.; Qiu, G. L.; Anderson, C. W.; Yao, H. *Environ. Sci. Technol.* **2012**, *46*, 11013−11020.
(35) Clarisse, O.; Dimock, B.; Hintelmann, H.; Best, E. P. *Environ. Sci. Technol.* **2011**, *45*, 1506−1512.
(36) Hong, Y. S.; Rifkin, E.; Bouwer, E. J. *Environ. Sci. Technol.* **2011**, *45*, 6429−6436.
(37) USEPA. *Guidance for Implementation and Use of EPA Method 1631 for the Determination of Low-Level Mercury*; USEPA, 2001.
(38) Shi, X. Y.; Fang, W.; Tang, N.; Williams, P. N.; Hu, X.; Liu, Z. D.; Yin, D. X.; Ma, L. Q.; Luo, J. *Environ. Sci. Technol.* **2018**, *52*, 14140−14148.
(39) Docekalova, H.; Divis, P. *Talanta* **2005**, *65*, 1174−1178.
(40) Wagner, S.; Santner, J.; Irrgeher, J.; Puschenreiter, M.; Happel, S.; Prohaska, T. *Anal. Chem.* **2022**, *94*, 6338−6346.
(41) Zhao, L.; Qiu, G. L.; Anderson, C. W. N.; Meng, B.; Wang, D. Y.; Shang, L. H.; Yan, H. Y.; Feng, X. B. *Environ. Pollut.* **2016**, *215*, 1−9.
(42) Rosera, T. J.; Janssen, S. E.; Tate, M. T.; Lepak, R. F.; Ogorek, J. M.; DeWild, J. F.; Krabbenhoft, D. P.; Hurley, J. P. *ACS ES&T Water* **2022**, *2*, 701−709.
(43) Xia, J.; Wang, J.; Zhang, L.; Wang, X.; Yuan, W.; Peng, T.; Zheng, L.; Tian, W.; Feng, X. *Water Res.* **2022**, *226*, 119271.
(44) Yin, R. S.; Feng, X. B.; Meng, B. *Environ. Sci. Technol.* **2013**, *47*, 2238−2245.
(45) Yan, H. Y.; Feng, X. B.; Shang, L. H.; Qiu, G. L.; Dai, Q. J.; Wang, S. F.; Hou, Y. M. *Sci. Total Environ.* **2008**, *407*, 497−506.
(46) Li, P.; Feng, X. B.; Shang, L. H.; Qiu, G. L.; Meng, B.; Liang, P.; Zhang, H. *Appl. Geochem.* **2008**, *23*, 2055−2064.
(47) Yin, R. S.; Krabbenhoft, D. P.; Bergquist, B. A.; Zheng, W.; Lepak, R. F.; Hurley, J. P. *J. Anal. At. Spectrom.* **2016**, *31*, 2060−2068.
(48) Blum, J. D.; Bergquist, B. A. *Anal. Bioanal. Chem.* **2007**, *388*, 353−359.
(49) Fang, W.; Yang, Y.; Williams, P. N.; Sun, H. T.; Chen, H. Y.; Yang, D. X.; Shi, X. Y.; Fu, R. B.; Luo, J. *Anal. Chem.* **2022**, *94*, 4576−4583.
(50) Muller, A. L.; Oliveira, J. S.; Mello, P. A.; Muller, E. I.; Flores, E. M. *Talanta* **2015**, *136*, 161−169.
(51) Fang, W.; Shi, X. Y.; Yang, D. X.; Hu, X.; Williams, P. N.; Shi, B. Q.; Liu, Z. D.; Luo, J. *Anal. Chem.* **2020**, *92*, 3581−3588.
(52) Fang, Z.; Li, K. X.; Li, Y.; Zhang, H.; Jones, K. C.; Liu, X. Y.; Liu, S. Y.; Ma, L. Q.; Luo, J. *Environ. Sci. Technol.* **2019**, *53*, 11223−11231.
(53) Zou, Y. T.; Fang, Z.; Li, Y.; Wang, R.; Zhang, H.; Jones, K. C.; Cui, X. Y.; Shi, X. Y.; Yin, D.; Li, C.; Liu, Z. D.; Ma, L. Q.; Luo, J. *Anal. Chem.* **2018**, *90*, 10016−10023.
(54) Destro Colaço, C.; Nozomi Marques Yabuki, L.; Marta Rolisola, A.; Antonio Menegário, A.; de Almeida, E.; Alfredo Suárez, C.; Gao, Y.; Corns, W. T.; do Nascimento Filho, V. F. *Talanta* **2014**, *129*, 417−421.
(55) Ren, M. Y.; Wang, Y.; Ding, S. M.; Yang, L. Y.; Sun, Q.; Zhang, L. P. *New J. Chem.* **2018**, *42*, 7976−7983.
(56) Reichstadter, M.; Divis, P.; Abdulbur-Alfakhoury, E.; Gao, Y. *Talanta* **2020**, *217*, 121059.
(57) Fang, Z.; Li, Y.; Li, Y. Y.; Yang, D. X.; Zhang, H.; Jones, K. C.; Gu, C.; Luo, J. *Environ. Sci. Technol.* **2021**, *55*, 9548−9556.
(58) Hanousek, O.; Santner, J.; Mason, S.; Berger, T. W.; Wenzel, W. W.; Prohaska, T. *Anal. Bioanal. Chem.* **2016**, *408*, 8333−8341.
(59) Chen, W.; Pan, S.; Cheng, H.; Sweetman, A. J.; Zhang, H.; Jones, K. C. *Water Res.* **2018**, *137*, 211−219.
(60) Deng, H. M.; Luo, M. T.; Shi, X. Y.; Williams, P. N.; Li, K. X.; Liu, M. L.; Fan, W. Y.; Xiao, T. F.; Chen, Y. H.; Ma, L. Q.; Luo, J. *Anal. Chem.* **2018**, *91*, 1344−1352.
(61) Zhang, H.; Davison, W. *Anal. Chem.* **1995**, *67*, 3391−3400.
(62) Bennett, W. W.; Teasdale, P. R.; Panther, J. G.; Welsh, D. T.; Jolley, D. F. *Anal. Chem.* **2010**, *82*, 7401−7407.
(63) Davison, W. *Diffusive Gradients in Thin-Films for Environmental Measurements*; Cambridge University Press, 2016, pp 149−150.
(64) Gao, L.; Gao, B.; Yin, S.; Xu, D.; Gao, J. *Chemosphere* **2018**, *195*, 390−397.
(65) Panther, J. G.; Teasdale, P. R.; Bennett, W. W.; Welsh, D. T.; Zhao, H. *Anal. Chim. Acta* **2011**, *698*, 20−26.
(66) Bland, G. D.; Rao, B.; Reible, D. *Sci. Total Environ.* **2020**, *749*, 141217.

https://doi.org/10.1021/acs.analchem.3c01356
Anal. Chem. 2023, 95, 12290−12297